Supplementary File

Carbon nanotube incorporated magnetic biochar derived from water hyacinth for chromium removal from tannery effluent

M. Hedayet Ullah[1,2], Mohammad Jellur Rahman[1*]

[1] Department of Physics, Bangladesh University of Engineering and Technology, Dhaka-1000, Bangladesh

[2] Department of Physics, Bangladesh University of Textiles, Dhaka-1208, Bangladesh

**Corresponding Author*: Mohammad Jellur Rahman (Email: mjrahman@phy.buet.ac.bd)

First Author: M. Hedayet Ullah (hedayet@phy.butex.edu.bd)

2.5. *Characterization*

The surface morphology of the raw WHB and the nanocomposite are characterized using field-emission scanning electron microscopy (FE-SEM, Zeiss Sigma 300VP, Germany) and transmission electron microscopy (TEM, Talos F200X G2, Thermo Fisher Scientific). A BET Sorptometer (BET-201-A, PMI, USA) is used to measure the surface areas. The chemical structure of the synthesized samples is identified using a double-beam FTIR spectrometer (Shimadzu, FTIR-8400) with wave numbers ranging from 400 to 4000 cm^{-1} and a resolution of 2 cm^{-1}. The crystalline phases of the nanocomposite are characterized using powder X-ray diffraction (XRD) analysis, performed on a Philips X'Pert PW 3040 diffractometer (Netherlands) with CuKα radiation over a 2θ range of 10° to 90°. X-ray photoelectron spectroscopy (XPS) is performed with a Kα spectrometer to analyze the chemical states of the elements. The total Cr concentration in the contaminated water is measured by atomic absorption spectroscopy (AAS, iCE 3000 series, USA).

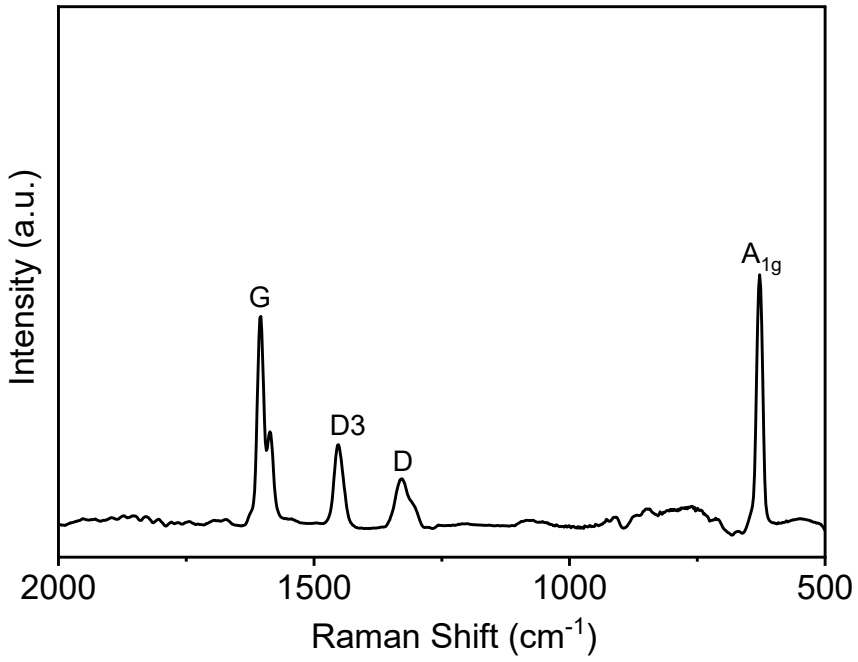

Fig. S1 Raman spectrum of CNT-CZB nanocomposite at room temperature.

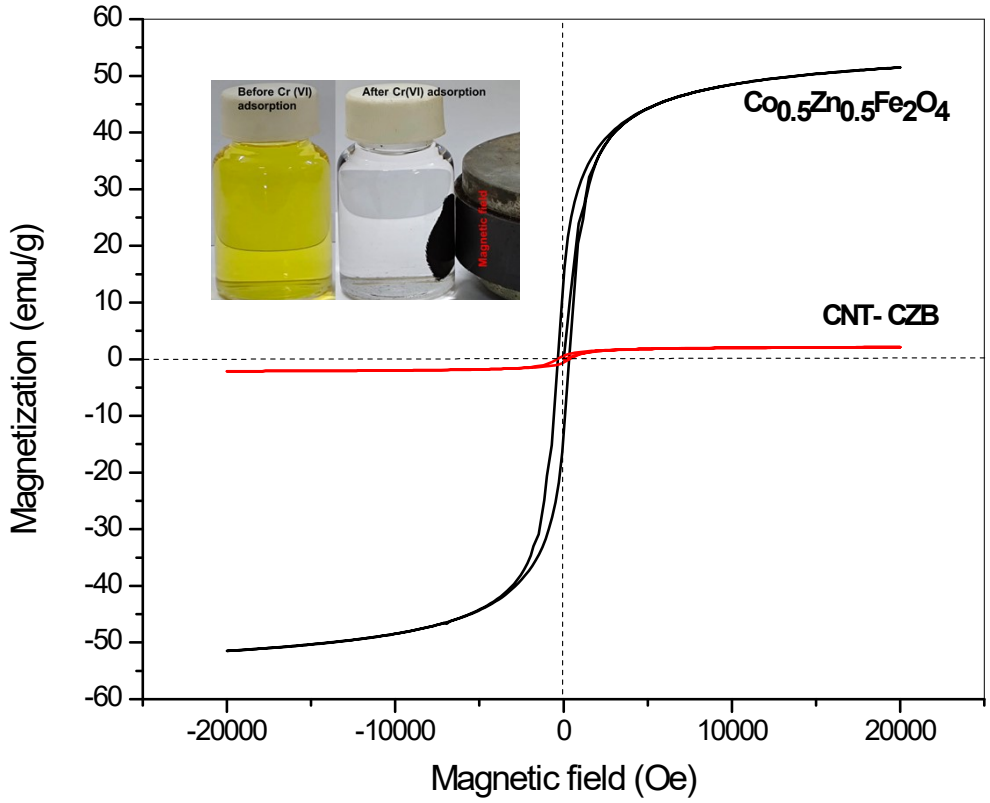

Fig. S2 Magnetization curve for Co-Zn ferrite and CNT-CZB nanocomposite.

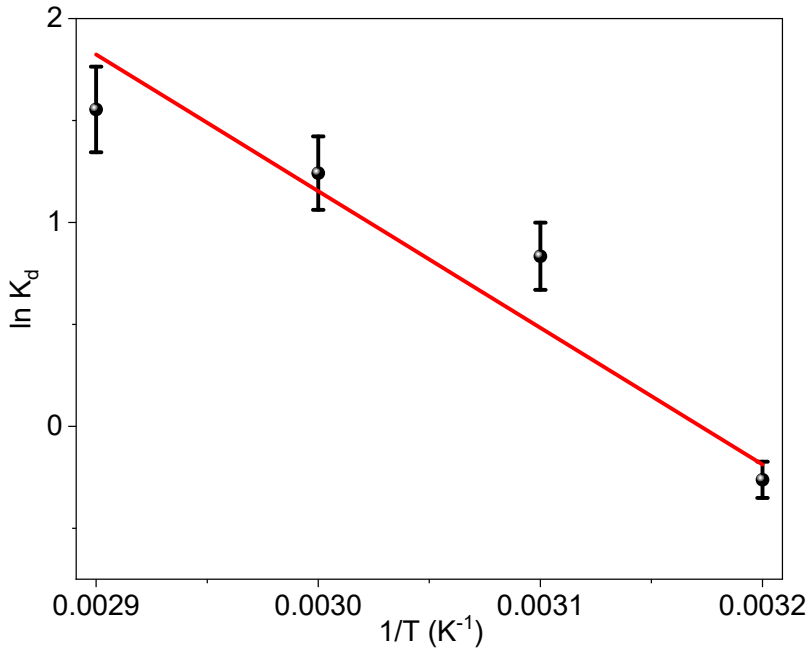

Fig. S3 A plot of lnK_d versus $1/T$ to estimate the thermodynamic parameters for Cr adsorption on the CNT-CZB nanocomposite.

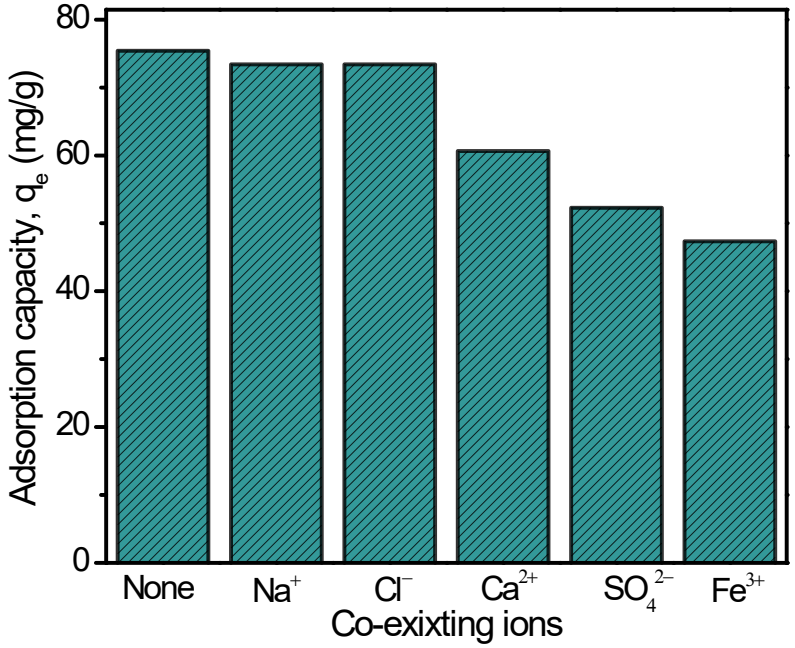

Fig. S4 Effect of co-existing ions on the adsorption capacity of Cr.

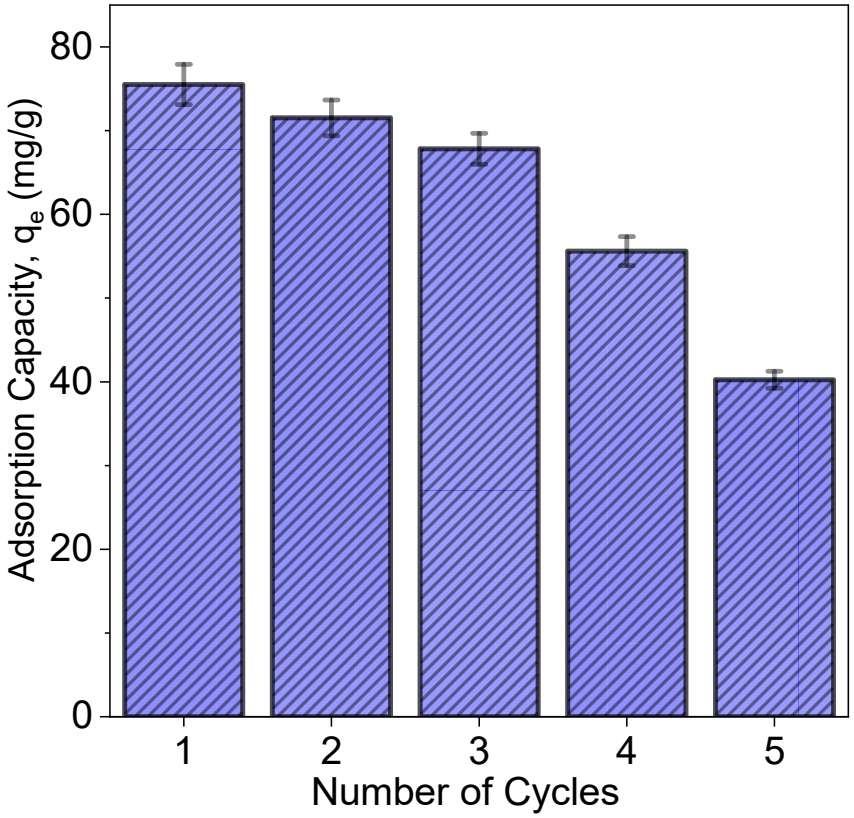

Fig. S5 Reusability study of CNT-CZB composite.

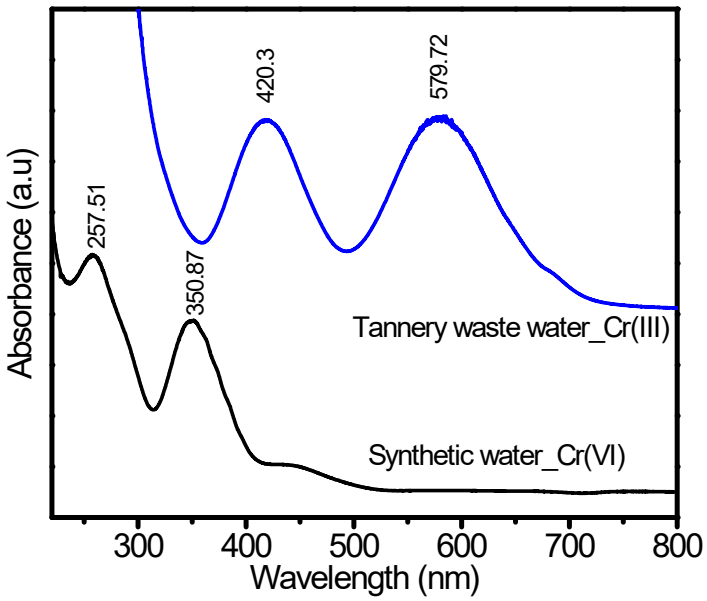

Fig. S6 UV-Vis spectra of the synthetic sample and tannery wastewater.

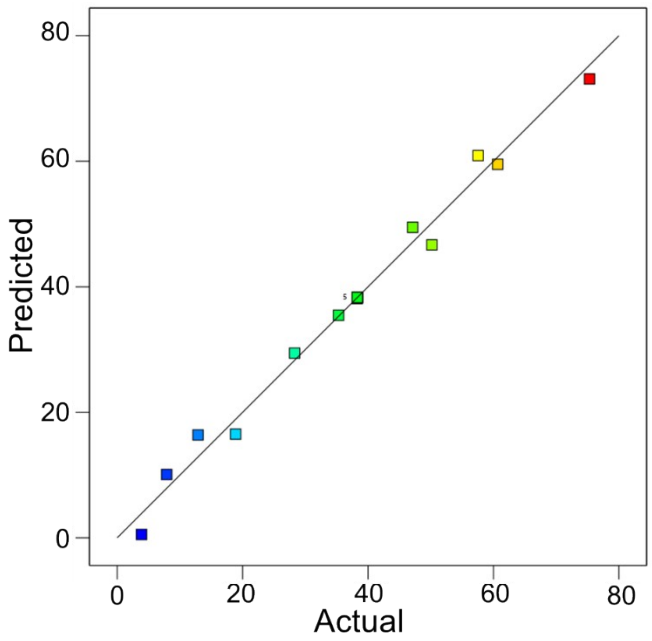

Fig. S7 Actual and predicted values of the model for Cr adsorption capacity.

Table S1 Parameters associated with different kinetic models for Cr adsorption.

Model	Parameters	*a*-WHB	CNT-CZB	Interpretation
PFO	$q_{m,\,exp}$ (mg/g)	44.58 ± 1.41	78.12 ± 1.58	The adsorption process is dominated by physical adsorption or surface diffusion.
	$q_{m,\,cal}$ (mg/g)	43.62 ± 0.70	74.28 ± 1.60	
	k_1 (min^{-1})	0.051 ± 0.002	0.168 ± 0.017	
	R^2	0.993	0.955	
	Adj R^2	0.992	0.944	
	χ^2	2.143	8.983	
	RSS	15.005	35.933	
PSO	$q_{m,\,exp}$ (mg/g)	44.58 ± 1.41	78.12 ± 1.58	Adsorption is primarily chemically controlled.
	$q_{m,\,cal}$ (mg/g)	49.61±0.74	80.62 ± 0.563	
	k_2 (g/mg.min)	0.002 ± 0.00007	0.003 ± 0.00001	
	R^2	0.996	0.995	
	Adj R^2	0.995	0.994	
	χ^2	1.157	0.939	
	RSS	8.101	3.757	
Elovich	α (mg/g.min)	5.22 ±1.41	4.85 ± 3.03	Heterogeneous surface with a reasonably high initial adsorption rate.
	β (g/mg)	0.096 ± 0.01	0.118 ± 0.01	
	R^2	0.958	0.917	
	Adj R^2	0.952	0.897	
	χ^2	2.311	16.553	
	RSS	13.871	66.214	

Table S2 Parameters associated with the different isotherm models for Cr adsorption on WHB and CNT-CZB.

Model	Parameters	*a*-WHB	CNT-CZB	Interpretation
Langmuir	$q_{m,\,exp}$ (mg/g)	43.12 ± 4.75	79.80 ± 3.99	Monolayer adsorption on a homogeneous surface.
	$q_{m,\,cal}$ (mg/g)	41.22 ± 2.9	111.82 ± 39.21	
	k_L (L/mg)	1.69 ± 0.27	0.014 ± 0.007	
	R^2	0.980	0.873	
	Adj R^2	0.969	0.855	
	χ^2	1.58	24.47	
	RSS	7.93	171.31	
Freundlich	n	0.34 ± 0.04	0.7 ± 0.13	Multilayer adsorption on heterogeneous surfaces.
	k_F (L/mg)	9.38 ± 1.66	2.84 ± 1.69	
	R^2	0.878	0.797	
	Adj R^2	0.854	0.768	
	χ^2	7.65	39.30	
	RSS	38.25	275.16	
Sips	$q_{m,\,exp}$ (mg/g)	43.04	79.80 ± 3.99	Mixed adsorption mechanisms.
	$q_{m,\,cal}$ (mg/g)	40.35 ± 2.57	78.93 ± 3.71	
	k (L/mg)	3.59 ± 1.82	0.08 ± 0.005	
	n	1.26 ± 0.17	2.51 ± 0.26	
	R^2	0.983	0.988	
	Adj R^2	0.975	0.985	
	χ^2	1.27	15.12	
	RSS	5.11	2.52	

Table S3 Experimental design and results for Box-Behnken design (BBD)

Run	Code levels			Conditions			Adsorption Capacity (mg/g)	
				pH	Initial Concentration (mg/L)	Time (min)	Actual	Predicted
1	1	0	-1	10	165	20	28.29	29.44
2	0	-1	-1	6	10	20	3.8896	0.54
3	0	0	0	6	165	100	38.3	38.70
4	-1	0	-1	2	165	20	38.29	38.12
5	-1	-1	0	2	10	100	12.9	16.4
6	0	0	0	6	165	100	38.3	38.3
7	0	0	0	6	165	100	38.3	38.3
8	-1	0	1	2	165	180	60.68	59.52
9	0	0	0	6	165	100	38.3	38.3
10	0	1	-1	6	320	20	47.12	49.47
11	1	1	0	10	320	100	50.19	46.68
12	0	0	0	6	165	100	38.3	38.3
13	1	-1	0	10	10	100	7.896	10.09
14	-1	1	0	2	320	100	75.32	73.12
15	0	-1	1	6	10	180	18.89	16.53
16	0	1	1	6	320	180	57.56	60.90
17	1	0	1	10	165	180	35.3	35.46

Table S4 ANOVA for Box-Behnken Design for Cr adsorption capacity by CNT-CZB nanocomposite.

Source	Sum of Squares	df	Mean Square	F-value	p-value	Remarks
Model	5598.72	9	622.08	61.80	< 0.0001	Significant
X_1	536.51	1	536.51	53.30	0.0002	
X_2	4353.12	1	4353.12	432.49	< 0.0001	
X_3	375.93	1	375.93	37.35	0.0005	
X_1X_2	101.26	1	101.26	10.06	0.0157	
X_1X_3	59.14	1	59.14	5.88	0.0458	
X_2X_3	5.20	1	5.20	0.5166	0.4956	
X_1^2	52.34	1	52.34	5.20	0.0566	
X_2^2	116.02	1	116.02	11.53	0.0115	
X_3^2	5.92	1	5.92	0.5882	0.4682	
Residual	70.46	7	10.07			
Lack of Fit	70.46	3	23.49			
Pure Error	0.0000	4	0.0000			
Cor Total	5669.18	16				

Supplementary File

Table S5 Model summary statistics.

Source	p-Value	AIC	BIC	Adjusted R^2	Predicted R^2	Remarks
Linear	< 0.0001	110.9	113.42	0.9124	0.8526	
2FI	0.1373	107.11	112.94	0.9328	0.7909	
Quadratic	0.0288	92.41	100.75	0.9716	0.8011	Suggested

Table S6 Fit statistics for the quadratic model.

Parameter	Value	Parameter	Value
Std. Dev.	3.17	R^2	0.9876
Mean	36.93	Adjusted R^2	0.9716
C.V. %	8.59	Predicted R^2	0.8011
		Adeq Precision	29.8287